Potential fluctuations due to inhomogeneity in hydrogenated amorphous silicon and the resulting charged dangling-bond defects

Howard M. Branz
Solar Energy Research Institute, Golden, Colorado 80401

Marvin Silver
University of North Carolina, Chapel Hill, North Carolina 27514
(Received 27 November 1989; revised manuscript received 25 May 1990)

We consider the thermodynamic equilibrium statistics of the "dangling-bond" undercoordination defect in undoped hydrogenated amorphous silicon (*a*-Si:H), assuming that material inhomogeneity causes electrostatic potential fluctuations whose peak-to-peak magnitude is greater than the (positive) effective correlation energy. We show that the fluctuations cause the formation of significant concentrations of charged dangling-bond defects. The negative defects form in regions of high potential and have transition energies below the Fermi energy (E_F). The positive defects form in regions of low potential and have transitions above E_F. We discuss evidence for the model and consequences of the charged dangling-bond defects for electron-spin resonance, transport, and photostability in *a*-Si:H.

I. INTRODUCTION

Bar-Yam *et al.*[1] showed that a distribution of thermodynamic transition energy levels of the threefold-coordinated Si "dangling-bond" defect, T_3, can lead to significant concentrations of the charged defects T_3^- and T_3^+ in inhomogeneous hydrogenated amorphous silicon (*a*-Si:H), *even with a positive effective correlation energy,* $U_{\rm eff}$. The T_3^- have $(-/0)$ thermodynamic transition levels below the Fermi level (E_F) and the T_3^+ have $(0/+)$ levels above E_F. In this paper, we show that electrostatic potential fluctuations of peak-to-peak magnitude greater than $U_{\rm eff}$ lead to similar phenomena and illustrate the physics involved. Ours is a "defect pool" model closely related to those of Smith[2] and of the Winer and Street group[3] because we assume, as they do, that defect equilibration occurs in *inhomogeneous* *a*-Si:H. We describe the origin of the potential fluctuations, calculate the density of electronic states predicted by the theory, and present experimental evidence that this model is applicable to *a*-Si:H.

II. POTENTIAL FLUCTUATIONS

Random potential fluctuations have been used to explain many phenomena in amorphous semiconductors including the mobility edge and band tails[4,5] and various transport phenomena.[6] Such fluctuations were first introduced to treat transport in heavily doped crystalline semiconductors.[7,8] More recently, potential fluctuations with a root-mean-square (rms) deviation of $V_{\rm rms} \sim 0.6$ eV were shown to arise from inclusion of 15% H at random in a crystal-Si matrix.[9]

We consider here fluctuations created by dipolar or higher-order charge distributions associated with material inhomogeneity. In the *a*-Si:H continuous density of states, random monopoles are screened by defects with levels near the Fermi level to yield small ($\lesssim 100$ meV) fluctuations with a correlation length of 100 to 500 Å (Ref. 10). Because the potential of a dipole falls like r^{-2}, it cannot be effectively screened by the continuous density of states, and a random array of dipoles yields short-range, intense potential fluctuations.[11] This is also true of higher-order multipolar charge distributions. Inhomogeneous *a*-Si:H contains several sources of dipolar or higher-order potential fluctuations.

The dipoles formed by charge transfer between Si and H are likely the most important source of short-range potential fluctuations. There are $\sim 5\times 10^{21}$ cm^{-3} Si—H bonds in *a*-Si:H, which contains 10 at. % of H. Ley *et al.*[12] estimate from photoemission experiments on *a*-Si:H that about 0.15 electron shifts from a Si atom to each H bonded to it. This experimental result is supported by studies of gaseous Si compounds[13] and by theoretical calculations.[14] The charge transfer means that each Si—H bond is a dipole of about 1.1 D. With the *a*-Si:H bulk dielectric constant $\epsilon = 12$, the potential magnitude due to one such dipole is 57 meV at a distance of 2.3 Å from the bond center (1.5 Å from the H or Si atom) along the dipolar axis. This potential falls roughly as r^{-2}, even at short distances (e.g., to 30 meV at 3 Å). At short distances the dielectric screening due to bond charge is likely reduced and the effective dielectric constant may be considerably less than 12. The actual potential due to the Si-H dipoles would then be greater than the values we quote above.

Multiple quantum nuclear-magnetic-resonance (MQNMR) studies[15] show that about two-thirds of the Si-H dipoles cluster in groups of four to eight dipoles with each hydrogen no more than 3 Å from its nearest neighbor H. Yet infrared absorption (ir) studies of the same samples demonstrate that these clustered H are not associated with SiH_2 or $(SiH_2)_n$ bonding.[16] If Si-H dipole directions are random within each cluster, we expect their potentials to add at some Si sites and cancel at others. Potential fluctuations of over 100 meV (rms) with a

correlation length of order 10 Å may result.

Static charge fluctuations between Si atoms due to bond-length and bond-angle disorder[17] have also been observed by photoemission[12] and by ^{29}Si NMR.[18] The rms charge fluctuations are about 0.08 and 0.11 electrons in a-Si:H and a-Si, respectively.[12] This corresponds to a rms dipole moment of about 0.8 D. These dipoles are slightly smaller and presumably less clustered than the Si-H dipoles, but they are high density ($\sim 5\times 10^{22}$ cm^{-3}).

Oxygen is found at densities of at least 10^{18} cm^{-3} in a-Si:H and must therefore contribute to the electrostatic potential fluctuations. From the Pauling electronegativity scale, we estimate the dipole moment of an oxygen impurity bonded to two Si atoms as about 2 D, twice that of the Si—H bond. This is roughly equal to the dipole moment of H_2O, which has a slightly smaller electronegativity difference between the constituent atoms but a narrower bond angle. Other impurities, such as C and N, are also present but the electronegativity difference between C and Si is small and the Si_3N grouping is quite symmetric, so their dipole moments can be ignored.

Recent small-angle x-ray-scattering (SAXS) results[19] show that even device-quality a-Si:H contains roughly 5×10^{19} cm^{-3} microvoids of 15–20 missing atoms. Any inhomogeneity of dielectric constant will result in an electrostatic potential felt by a test charge due to induced dipoles at the inhomogeneity boundary. The resulting potential may be calculated by the method of image charge.[20] For example, the potential felt by a positive test charge 2.3 Å from a void is about 100 meV and by a negative test charge is about -100 meV. This is another source of potential fluctuations.

There are evidently many forms of local inhomogeneity in a-Si:H, including Si—H bonds, clustered Si—H bonds, impurities, microvoids, position-dependent dielectric constant, and static charge fluctuations due to short-range disorder. Each of these forms of inhomogeneity can give rise to dipolar or higher-order potential fluctuations that cannot be screened by the continuous density of states near the Fermi level. In this paper, we consider the effects of these short- to medium-range (5–30 Å), intense, potential fluctuations on defect densities in a-Si:H.

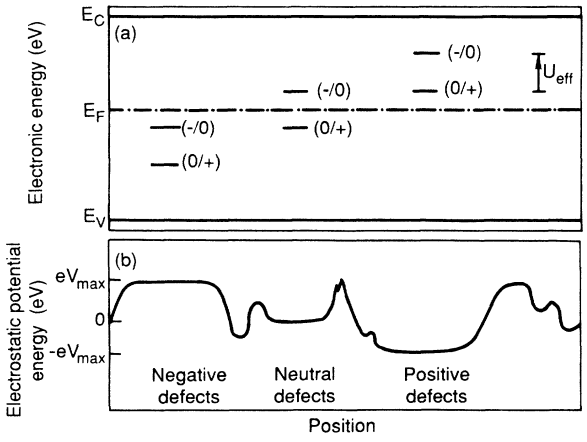

FIG. 1. The effect of a random electrostatic potential. (a) E_c, E_v, E_F, and the thermodynamic transition levels of the dangling-bond defect in regions of different potential. (b) The electrostatic potential energy of a positive test charge in the corresponding regions.

Figure 1 is a schematic diagram of relevant electronic energies in a-Si:H in these random potential fluctuations. Despite the potential fluctuations, the Fermi level (electron chemical potential) is by definition position independent at electronic equilibrium. The conduction- and valence-band mobility edges E_c and E_v, like E_F, do not depend on the electrostatic potential at the positions x, $V(x)$. The mobility edges are not position dependent in three-dimensional[21] potential fluctuations because they separate "extended" electronic states from localized states. The mobility edge can be viewed[5] as a percolation threshold at which carriers can transport throughout the material in dc-conductivity experiments[22] with no thermal excitation. As such, it is a position-independent energy.

III. THERMODYNAMICS OF DANGLING BONDS

Although a-Si:H growth is a nonequilibrium process, thermodynamics within an ensemble of accessible structures appears applicable to the structural defects.[1–3] Recent evidence[3,23–26] suggests that defects are found in concentrations which reflect a frozen-in thermodynamic equilibrium characteristic of a history-dependent temperature, $T^*\sim 200$ °C. We assume that structural relaxations are frozen out below T^*, i.e., kinetic barriers to defect creation and annihilation cannot be overcome on experimental time scales. Consequently, the concentration of the dangling-bond defect, T_3^q, frozen in at T^* is

$$n(T_3^q)=n_{\mathrm{Si}}\exp(-F[T_3^q]/kT^*)\ , \tag{1}$$

where n_{Si} is the density of Si atoms available to form dangling bonds. The formation energy F of a defect is the increase in total energy of the solid when the defect is introduced. As the system is cooled below T^*, the electronic distribution continues to equilibrate, but this has little effect on the dangling-bond concentration.[27] The density of defects is out of equilibrium below T^*, but there is no comparable kinetic barrier to electronic equilibration and the electronic level occupation follows the Fermi-Dirac distribution at all temperatures.

The formation energies of charged defects depend upon $V(x)$ but those of neutral defects do not. Thus, $F[T_3^0]$ is independent of $V(x)$ and the formation energies of the charged dangling bonds are

$$F[T_3^+,V(x)]=F_0[T_3^+]+eV(x)$$

and (2)

$$F[T_3^-,V(x)]=F_0[T_3^-]-eV(x)\ ,$$

where e is the electronic charge and F_0 is the formation energy of a defect at $V=0$, the mean value of $V(x)$. Already, we see that when thermodynamic equilibrium is established there will be a tendency to form defects of different charge states in different regions.

We next examine the dependence on E_F of the formation energies, $F_0[T_3^q,E_F]$, in homogeneous material

without potential fluctuations ($V=0$, everywhere), following Shockley and Moll[28] and Froyen and Zunger.[29] $F_0[T_3^0]$ is independent of E_F. For the charged defects

$$F_0[T_3^+,E_F]=F_0[T_3^0]+E_F-E_0(0/+)$$

and (3)

$$F_0[T_3^-,E_F]=F_0[T_3^0]+E_0(-/0)-E_F\ .$$

The last two terms of each equation represent the energy needed to move an electron (or hole) from the neutral defect to the Fermi sea. Figure 2(a) exhibits the formation energies and the logarithmic concentrations at T^* of the dangling-bond defects. $E_0(r/s)$ is the thermodynamic transition level from state r to state s, for $V=0$. By definition, when $E_F=E_0(-/0)$, the formation energy $F_0[T_3^0]=F_0[T_3^-]$ and a defect converts freely between the two charge states. Experiments such as deep-level transient spectroscopy (DLTS) (assuming thermal carrier emission is accompanied by complete defect relaxation) measure the energy difference between $E_0(r/s)$ and a band mobility edge. The correlation energy is $U_{\rm eff}=E_0(-/0)-E_0(0/+)$. The thermodynamic transition levels $E_0(0/+)$ and $E_0(-/0)$ correspond to the usual one-electron levels D^0 and D^-, respectively. The corresponding effective density of one-electron levels is shown in Fig. 2(b) for undoped homogeneous a-Si:H.

To model the inhomogeneous material, we substitute Eqs. (3) into Eqs. (2) and find the formation energies F in the presence of potential fluctuations $V(x)$. The formation energy of the neutral defect, $F[T_3^0]$, is independent of both $V(x)$ and E_F. For the charged defects

$$F[T_3^+,E_F,V(x)]=F[T_3^0]+E_F-E_0(0/+)+eV(x)$$

and (4)

$$F[T_3^-,E_F,V(x)]=F[T_3^0]+E_0(-/0)-E_F-eV(x)\ .$$

The actual thermodynamic transition levels at x, $E(0/+)$ and $E(-/0)$, occur at those values of E_F for which $F[T_3^0]=F[T_3^+]$ and $F[T_3^-]=F[T_3^0]$, respectively. Substituting these expressions into Eqs. (4) and solving for E_F yields

$$E(0/+)=E_0(0/+)-eV(x)$$

and (5)

$$E(-/0)=E_0(-/0)-eV(x)\ .$$

The effect of potential fluctuations on the transition levels, assuming a position-independent, positive value of $U_{\rm eff}$, is pictured in Fig. 1(a). If the maximum value of $eV(x)$, $eV_{\rm max}$, is greater than $U_{\rm eff}/2$, there will be $(-/0)$ transition levels below E_F and $(0/+)$ transition levels above E_F. Charged dangling-bond defects result.

Figure 3(a) shows the formation energies and logarithmic concentrations of T_3^+, T_3^-, and T_3^0 as functions of E_F. The dashed lines represent T_3^- defects in the regions of minimum and maximum potential. The minimum corresponding transition level $E(-/0)_{\rm min}$ and the $V=0$ transition level $E_0(-/0)$ are also shown in Fig. 3.

From the simple relations among potential, formation

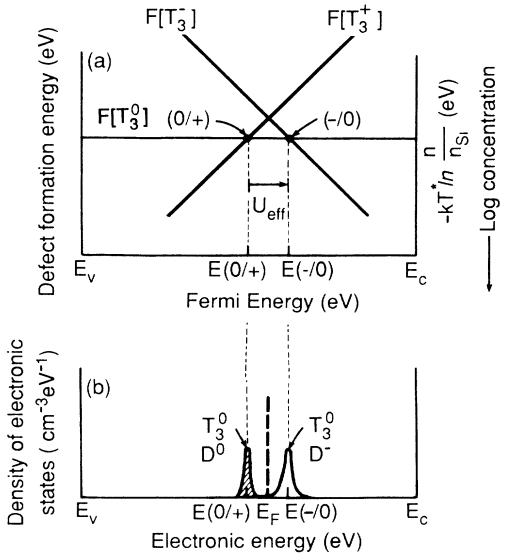

FIG. 2. Formation energies (up) and concentrations at T^* (down) of relaxed dangling bonds as functions of E_F in the absence of potential fluctuations. (b) Corresponding electronic density-of-states diagram for undoped a-Si:H. States are labeled by T_3^0, the defect with which they are associated. The labels D^0 and D^-, sometimes found in the literature, are also given. The filled state is shaded.

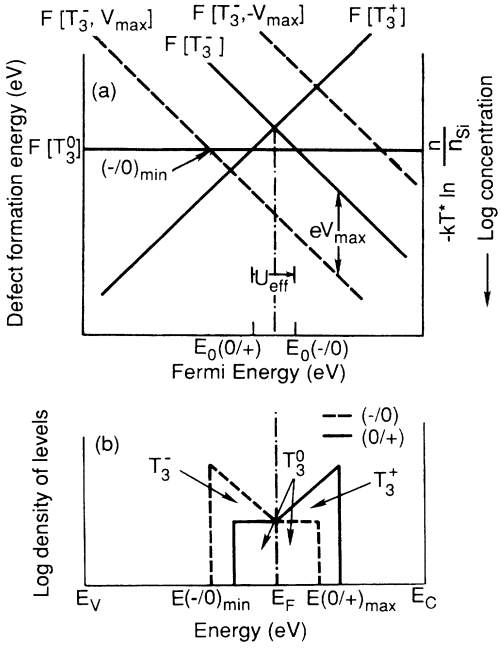

FIG. 3. (a) Formation energies of T_3^+ at $V=0$ and of T_3^- at $V=0$, $V_{\rm max}$, and $-V_{\rm max}$ as functions of E_F. (b) The densities of thermodynamic transition levels of T_3^+, T_3^-, and T_3^0 defects for the flat potential distribution with $eV_{\rm max}=2U_{\rm eff}$ described in the text. The actual value of E_F is indicated.

energies, and transition levels which are depicted graphically in Fig. 3(a), the density of thermodynamic (electronic) transition levels can be calculated for a given potential fluctuation distribution function. The simplest case is that of a flat potential distribution function, and Fig. 3(b) shows the logarithmic density of electronic transition levels (density of states) for this distribution. To construct Fig. 3(b), we assume the potential fluctuations are distributed such that each value of potential between $-V_{\max}$ and $V_{\max}$ is found in the same fractional volume of the solid and that $eV_{\max}=2U_{\text{eff}}$. The dashed line is the density of $(-/0)$ transition levels and the solid line is the density of $(0/+)$ levels. If there are no other charged defects in the solid, charge neutrality dictates that E_F is at the crossing point of $F_0[T_3^-,E_F]$ and $F_0[T_3^+,E_F]$, as pictured. Obviously, each $(-/0)$ level below E_F is associated with a T_3^- defect and each $(0/+)$ level above E_F is associated with a T_3^+ defect.

The T_3^+ and T_3^- defects are *not* spatially correlated. In regions of high potential, the lowest formation energy defects are T_3^- that have transition levels below midgap. Similarly, T_3^+ are formed in regions of low potential and have transition energies above midgap. The concentration of charged dangling-bond defects in regions with $|eV|>U_{\text{eff}}/2$ increases exponentially with $|eV|$ and there are no T_3^0 defects in these regions. This is shown schematically in Fig. 4.

It should be noted that there are not enough charged defects formed to neutralize the potential fluctuations. Even 10^{17} cm^{-3} of these defects (a high density compared to that of T_3^0 defects) corresponds to a probability of 10^{-3} that a defect forms in any particular 20 Å fluctuation. Further, a random distribution of charged defects gives rise to longer-range, smaller-magnitude potential fluctuations[8,10] which cannot cancel the dipolar fluctuations.

Only T_3^0 defects are found in regions with $|eV|<U_{\text{eff}}/2$. Each of these T_3^0 defects contributes both a $(-/0)$ level above E_F and a $(0/+)$ level below E_F to the density of electronic transition levels in Fig. 3(b).

Figure 5 shows the density of states predicted by our model for a more-realistic Gaussian distribution of potential fluctuations. In place of the approximate Eq. (2), we use a more-correct form[3] which continues to hold as the density of the defects approaches n_{Si}. Details of the calculation and the results for a variety of parameter sets are given elsewhere.[30] In Fig. 5, the Gaussian fluctuation full width is 0.3 eV, in approximate agreement with observed dangling-bond transition-level widths from optical absorption and luminescence experiments (see Sec. V). Other parameters are $U_{\text{eff}}=0.2$ eV (Ref. 31), $F[T_3^0]=0.3$ eV (Refs. 2, 3, and 26), $n_{\text{Si}}\sim10^{19}$ cm^{-3}, $kT^*=42$ meV (Ref. 25), and $E_F=E_V+1.0$ eV. The dashed curve shows the $(-/0)$ thermodynamic transitions levels. Integrating this curve below E_F yields a density of $\sim2\times10^{17}$ cm^{-3} T_3^- defects. Integrating the $(-/0)$ levels above E_F yields a density of $\sim8\times10^{15}$ cm^{-3} T_3^0 defects. The solid curve shows the $(0/+)$ transitions. Of course, there are $\sim2\times10^{17}$ cm^{-3} $(0/+)$ transitions above E_F from the T_3^+ defects and $\sim8\times10^{15}$ cm^{-3} transitions below E_F from the T_3^0 defects. Though the Gaussian potential distribution function smooths Fig. 5 relative to Fig. 3(b), the remaining sharp cutoffs are a consequence of our unphysical assumption that U_{eff} is precisely constant throughout inhomogeneous a-Si:H.

The transition levels shown in Figs. 3(b) and 5 are *thermodynamic* transition levels with their full structural relaxation. We expect the optical transition levels of the T_3^+ and T_3^- defects to be at least 0.2 eV closer to E_c and E_v, respectively.[27] This may bury the optical transition levels of T_3^+ and T_3^- in the band tails and render the charged dangling-bond defects unobservable in optical-absorption experiments.

Potential fluctuations are a simple physical model of how defect thermodynamic equilibrium and disorder give rise to charged dangling-bond defects in undoped a-Si:H in spite of a positive value of U_{eff}. Bar-Yam *et al.*[1] first proposed that a distribution of thermodynamic transition energies and a small U_{eff} would result in charged dangling-bond defects. Their model is based upon earlier total-energy calculations[32] showing that U_{eff} of the dangling bond is nearly independent of strainlike distortions applied to the host lattice, but the thermodynamic transi-

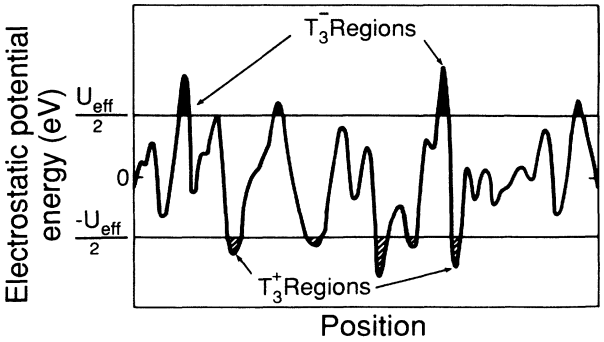

FIG. 4. Electrostatic potential energy of a positive test charge as a function of position in potential fluctuations. Regions with a high probability of forming charged dangling-bond defects are shaded. The maximum potential-energy fluctuations exceed $U_{\text{eff}}/2$.

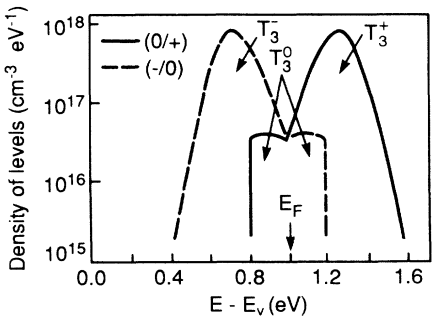

FIG. 5. Calculated densities of thermodynamic transition levels of T_3 defects for a Gaussian distribution of potential fluctuations. The fluctuation full width is 0.3 eV, U_{eff} is 0.2 eV, and other parameters are given in text.

tion levels $E(-/0)$ and $E(0/+)$ vary dramatically with the distortion. The phenomenology of a distribution of host distortions is therefore similar to that of our potential-fluctuation model.

Winer and Street[3] also propose a thermodynamic model of a-Si:H in which disorder gives rise to a distribution of defect thermodynamic transition levels in the gap and U_{eff} is a positive constant. The parameter that varies with position in their model is the "strain." They assume values of U_{eff} and of defect-band width (corresponding to the potential fluctuation width in the present model) which are similar to ours. Their model, however, does not predict that significant densities of charged dangling bonds form in undoped a-Si:H. Because the models and the parameters are somewhat different, it is difficult to compare the two approaches and isolate the reasons for their divergent conclusions about the defect densities. We will, however, make a few observations about the models.

The Winer-Street model[3] assumes that all defect formation energies are given by differences among one-electron energies of states in the a-Si:H energy gap. As a consequence, $F[T_3^+]$ is independent of the strain parameter in this model, while $F[T_3^0]$ has half the strain dependence of $F[T_3^-]$. The assumption that the defect formation energy equals a sum over all the one-electron energies of the valence electrons can be used to calculate the total energies of some crystals,[33] but may not be valid when large lattice relaxations occur as when breaking a Si—Si bond to form T_3^0. Further, by including only the energies of gap-state electrons, these authors ignore the energies of the three Si outer-shell electrons deep in the valence band.

The position independence of $F[T_3^+]$ may explain why the Winer-Street model predicts few charged dangling bonds. In contrast, $F[T_3^0]$ is position independent in our potential-fluctuation model, while charged-defect formation energies depend upon position. We believe this is more physically reasonable. Obviously, only experimentation can determine whether or not copious charged dangling bonds are present in intrinsic a-Si:H, so we continue with a discussion of experiments indicating their existence.

IV. EXPERIMENTAL EVIDENCE FOR CHARGED DANGLING-BOND DEFECTS

There are many phenomena that may be interpreted as arising from charged dangling-bond defects in undoped a-Si:H. Some of these were examined[34–36] in the context of negative U_{eff}. In contrast to purely negative U_{eff} models, however, the present model allows for the experimentally observed dangling-bond spin signal and unpinned Fermi energy in a-Si:H. In this section, the evidence for charged dangling-bond defects created by potential fluctuations is reviewed. While some of the transport results could be explained by other charged-defect species, the transition levels are generally consistent with the dangling-bond defects and little evidence for other charged midgap species has been obtained.

The most direct evidence for charged dangling-bond defects in a-Si:H comes from light-induced electron-spin-resonance (LESR) measurements. Of T_3^+, T_3^-, and T_3^0, only T_3^0 has an unpaired spin observable in dark ESR. This is identified with the $g=2.0055$ line.[37,38] As observed in doped a-Si:H,[39] light-induced excitation of an electron into T_3^+ or a hole into T_3^- will produce a T_3^0 with an unpaired spin. Because charged dangling-bond defects outnumber neutral dangling bonds at equilibrium, we predict an increase in the $g=2.0055$ ESR signal under illumination.

Using low-intensity (3 mW cm^{-2}) white light and separating the $g=2.0055$ LESR line from the $g=2.0044$ and 2.01 "band-tail" lines, Shimizu *et al.*[40] observed a light-induced increase in T_3^0 density. By measuring a series of films from 1 to 8 μm thick, they estimate a bulk charged dangling-bond defect density of over 10^{16} cm^{-3} in as-grown a-Si:H with 2.3×10^{15} cm^{-3} of T_3^0 defects. As the saturation of this LESR signal with light intensity is not reported, 10^{16} cm^{-3} represents a lower limit to the charged dangling-bond defect density.

Ristein *et al.*[41] measured the ir-LESR signal of undoped a-Si:H. One of us (H.B.) analyzes these results in detail elsewhere[42] and suggests ir-LESR provides evidence of copious bulk T_3^+ and T_3^- defects. By using ir excitation, direct band-to-band transitions are precluded and the $g=2.0048$ and 2.011 ESR lines are suppressed relative to the $g=2.0055$ T_3^0 line. While they do not resolve the narrow $g=2.0055$ and 2.0048 lines, Ristein *et al.*[41] find that in an 8-μm sample these narrow lines outnumber the broad hole resonance at $g=2.011$ by a 3:1 ratio. This ratio is a natural consequence of equal excitation rates of holes from T_3^+ and electrons from T_3^- if the T_3^+ and T_3^- densities are equal.[42] To explain the ir-LESR data with bulk T_3^+ and T_3^-, there must be *at least* 6×10^{16} cm^{-3} of T_3^+ and T_3^- in their sample, which contains only 1.5×10^{16} cm^{-3} of T_3^0 spins. Thinner samples also show evidence of bulk charged dangling-bond defects but may be dominated by the high density of near-surface LESR spins previously observed by Shimizu *et al.*[40]

The recent depletion-width-modulated ESR (DWM-ESR) experiment of Essick and Cohen[43] also provides evidence for numerous T_3^- defects in undoped a-Si:H. A capacitance structure is alternately depleted and filled at 1 Hz. The emitted charge and ESR signals are observed in a lock-in mode. Depletion reduces the $g=2.0055$ spin signal from T_3^0, but only one spin is destroyed for every six electrons emitted from below E_F. This ratio remains roughly constant as the temperature is raised from 320 to 360 K and electrons are emitted from deeper and deeper levels. With an emission prefactor of $\nu_0=10^{12}$ s^{-1}, the deepest emissions are from less than 0.15 eV below E_F. Essick and Cohen[43] suggest a near-zero value of U_{eff} to explain their experiments, but this is inconsistent with the observations that the T_3^0 ESR density follows a Curie-law dependence upon T from 90 to 300 K (Ref. 44) and up to 420 K (Ref. 31). We reconcile the ESR and DWM-ESR observations below by assuming $U_{\text{eff}}>0$ in inhomogeneous a-Si:H with many T_3^- defects present.

In the present model, symmetric potential fluctuations together with a greater density of charged dangling-bond

defects than of other charged defect and impurity species (E_F at the"charge-neutral" position) give rise to equal densities of (0/+) and (−/0) transition levels at E_F. Both Figs. 3(b) and 5 exhibit this equality, a consequence of Eqs. (1), (4), and (5). Depletion to below E_F then yields a roughly equal number of $T_3^- \rightarrow T_3^0$ and $T_3^0 \rightarrow T_3^+$ transitions and their effects on the modulated ESR cancel. Consequently, the DWM-ESR signal is small.

An accurate simulation of the DWM-ESR experiment would include the different attempt-to-escape frequencies ν_0 expected for emission from T_3^- and T_3^0. Because of Coulomb attraction, the electron capture-rate constant to a T_3^+ defect may be several orders of magnitude greater than to a T_3^0 defect. Therefore, detailed balance arguments imply that ν_0 is higher for emission from T_3^0 than from T_3^-. The demarcation energy $E_d = E_c - kT\ln(\nu_0 t_d)$ for level emptying during the depletion time t_d is deeper for (0/+) levels than for (−/0) levels. Detailed simulations of emission using a density of states like that of Fig. 5 is required for a more quantitative analysis of the DWM-ESR experiment.

We next argue that the charged dangling-bond defects act as carrier traps, while the T_3^0 defects are effective recombination centers. The dangling bond is a trivalent defect. Consequently, recombination can follow either of two pathways. Through the (−/0) level, T_3^0 traps an electron to become T_3^- and this traps a hole to become T_3^0 and complete a recombination. Using the (0/+) level pathway, the defect alternates between T_3^+ and T_3^0.

Trapping and emission of holes can also use either the (−/0) level or the (0/+) level. In hole trapping through (−/0), for example, the T_3^0 emits a hole to become T_3^- and captures a hole to become T_3^0. Trapping and emission of electrons can similarly proceed through either a (0/+) or (−/0) level.

In general, levels near midgap function as recombination centers, those near the conduction-band edge are electron traps, and those near the valence-band edge are hole traps. The exact energies that divide trap levels from recombination levels are the trap quasi-Fermi levels.[45] These depend on illumination intensity and temperature. Simmons and Taylor[45] showed that the trap quasi-Fermi levels also depend upon the trap species—the ratio of electron-to-hole–capture rate constants for the defect transition involved.

Evidently, (−/0) and (0/+) levels of the dangling bond are different trap species. For a given transition $(q/q+1)$, b_n is the rate constant for capture of an electron to T_3^{q+1} and b_p is the rate constant for capture of a hole to T_3^q. Because $b_n/b_p \ll 1$ for a (−/0) level, a (−/0) anywhere in the lower half of the gap is likely to act as a hole trap. Near and above midgap, a (−/0) level functions as a recombination center. For a small range of energy near the conduction-band edge, (−/0) is an electron trap. Conversely, $b_n/b_p \gg 1$ for the (0/+) level and those in the upper half of the gap will usually function as electron traps, while levels near and below midgap are recombination centers.

These trap quasi-Fermi levels are illustrated schematically in Fig. 6 and should be compared to the density of levels illustrated in Fig. 5. The levels of T_3^0 will be recombination centers under most conditions due to their positions in the gap. Those of T_3^+ and T_3^- will more often function as carrier traps. These differences between the transition levels of the charged and neutral T_3 defects are even greater when equilibrium hybridization is considered.[27]

Adler[34] proposed that charge trapping in T_3^+ and T_3^- defects is responsible for the light-induced metastabilities in *a*-Si:H. The metastable effects of light soaking include reduced photoconductivity[46] and an enhanced ESR signal from the T_3^0 defect.[47] Upon illumination, the T_3^+ and T_3^- capture photogenerated electrons and holes, respectively, and with a low probability rehybridize to T_3^0 defects in the sp^3 configuration. The spin signal rises and the photoconductivity falls because of these additional recombination centers. Annealing proceeds over a barrier to rehybridization of the metastable T_3^0 defects. The annealing of light-induced T_3^0 defects restores the ground states: T_3^+ in the sp^2 hybridization and T_3^- in the unhybridized s^2p^3 configuration in regions of low and high potential, respectively. In contrast, T_3^0 defects formed by thermal quenching are located in regions with $|eV| < U_{\text{eff}}/2$ and anneal back to the normally bonded T_4^0 configuration. Different annealing kinetics for light-induced and quenched-in T_3^0 defects are therefore expected.

Crandall[48] found that charge trapping is an integral step in the creation of light-induced defects in *a*-Si:H. He also observed distinct emission times for electrons and holes while annealing the metastable defects. These results suggest that photogenerated electrons and holes are trapped at separate sites (T_3^+ and T_3^- defects) from which they anneal at different rates.

The T_3^- would normally be expected to trap holes without reconfiguring into light-induced sp^3-T_3^0 defects. Hole traps which are 0.4–0.6 eV above E_v and which act to enhance the electron photoconductivity of undoped *a*-Si:H were observed by several workers. Vanier and Griffith[49] and Persans[50] each performed dual-beam pho-

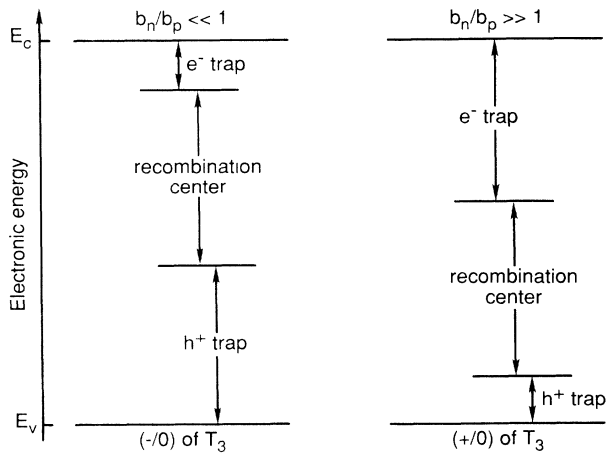

FIG. 6. Schematic diagram of the trap quasi-Fermi energies dividing T_3 traps from T_3 recombination centers during illumination.

toconductivity experiments to study these hole-trapping photoconductivity-sensitizing (s) centers. Vanier and Griffith[49] explain their data by assuming that the primary recombination centers have electron-capture cross sections at least 2000 times larger than those of the s centers. Persans[50] finds that the s centers have very small electron-capture coefficients, about 5×10^{-13} cm^3 s^{-1}. These results suggest that the s centers are the negative T_3^- defects while the primary recombination centers are the neutral T_3^0 centers.

McMahon and Crandall[51] investigated the s center and learned that the number of centers (which they call "safe-hole traps") diminishes during light soaking. Further, the numbers of s centers lost during soaking is comparable to the number of metastable T_3^0 defects created. We suggest these workers are observing the conversion of unhybridized s^2p^3-T_3^0 defects (s centers which have trapped a hole) into sp^3-hybridized T_3^0 defects (Staebler-Wronski defects). The hole trapping in an s center and its subsequent conversion to a metastable defect is expressed by

$$h^+ + T_3^-(s^2p^3) \overset{\text{HT}}{\longrightarrow} T_3^0(s^2p^3) \overset{R}{\longrightarrow} T_3^0(sp^3) ,$$

where HT denotes hole trapping and R denotes rehybridization. Annealing restores the s center[51] as it reduces the T_3^0 (sp^3) spin signal.[47] This model also explains the enhancement of ir absorption in a-Si:H due to absorption of intense visible light.[52] The visible light causes the s centers to capture holes and the ir radiation excites these holes to the valence band.[49]

It was suggested[51] that the s centers (safe-hole traps) may be the deep valence-band-tail states. We believe this is unlikely. A hole trapped in the valence-band tail is a positive T_4^+ center and is not safe. The T_4^+ has a Coulomb potential well which should increase its electron-capture coefficient above that of the T_3^0 recombination centers. In contrast, after hole trapping, the native T_3^- becomes neutral and can function as a safe-hole trap.

Charged scattering centers are known to reduce the electron extended state mobility, μ_e, in compensated a-Si:H[53,54] Similarly, the presence of T_3^- and T_3^+ defects could reduce μ_e in undoped a-Si:H. By experiments in which they apply an additional voltage plus to *p-i-n* and *metal-i-n* devices in forward bias, Xu *et al.*[55] find that under strong double injection of electrons and holes into a-Si:H, μ_e is substantially higher. They attribute this effect to defect neutralization of native charged defects by carrier trapping. Cannella *et al.*[36] previously observed that recombination-limited currents in *p-i-n* devices are 10^3 to 10^4 times larger than in an *n-i-n* device due to a dramatically reduced recombination coefficient of the electrons. They propose that the increased μ_e under double injection changes the mechanism of electron capture to recombination centers from a diffusive to a ballistic regime. Recently, Goldie *et al.*[56] found no significant enhancement of μ_e by time-of-flight experiments under double injection conditions, a result which confuses the experimental situation.

V. EXPERIMENTAL EVIDENCE FOR THE POTENTIAL FLUCTUATIONS

We showed in Sec. III that potential fluctuations are a simple model that yields distributions of thermodynamic transition energies. Charged dangling-bond defects will outnumber T_3^0 defects whenever the rms potential-energy fluctuations eV_{rms} are greater than $U_{\text{eff}}/2$. Significant numbers of charged defects also form with $eV_{\text{rms}} \lesssim U_{\text{eff}}/2$, because the distribution of fluctuations is not cut off at V_{rms} and the Boltzmann factor exponentially enhances the density of defects formed in regions of extreme potential [Eqs. (1) and (2)]. Wherever the maximum fluctuation eV_{max} exceeds $U_{\text{eff}}/2$, charged dangling-bond defects are formed.

Stutzmann and Jackson[31] find that $U_{\text{eff}}=0.2\pm0.1$ eV by analyzing ESR and other data. We described rough estimates of the dipole potential fluctuations in Sec. II. Several possible sources of 0.1–0.2 V rms potential fluctuations are present. We review below the experimental evidence that $eV_{\text{rms}} \gtrsim U_{\text{eff}}/2$ in a-Si:H.

It is widely observed that optical, luminescence, and DLTS energies are broadened in a-Si:H. The broadening reflects the distribution of transition levels caused by potential fluctuations. For example, Street[57] found dangling-bond defect-luminescence peak widths of about 0.4 eV in doped a-Si:H. Assuming that the optically ionized carrier rethermalizes to some well-defined energy prior to the luminescence transition, the width is due to a distribution of $(-/0)$ transition levels with $eV_{\text{rms}} \gtrsim 0.2$ eV. Other examples of broadened transitions are seen in optical-absorption experiments. Wronski *et al.*[58] and Kocka[59] fit optical-absorption data to Gaussian defect peaks with full widths ranging from 0.2 to 0.26 eV.

Another consequence of the distribution of transition levels is a deepening of the dominant optical-absorption transition level in doped a-Si:H.[1] An analysis of the experimental data that takes into account the vertical nature of optical transitions suggests that $eV_{\text{rms}} \sim 0.2$ eV.[27] This deepening is one component of the apparent deepening of charged dangling-bond-defect electronic levels in doped a-Si:H.[59] A second analysis of the data by Winer[3] suggests even more deepening and a broader distribution of local environments which we identify with potential fluctuations. Because $eV_{\text{rms}} \gtrsim U_{\text{eff}}/2$, there are significant regions of the undoped a-Si:H in which charged defects form at equilibrium.

VI. CONCLUSIONS

We have described the thermodynamic equilibrium statistics of positively correlated dangling-bond defects in inhomogeneous undoped a-Si:H. The electrostatic potential-fluctuation model yields thermodynamic transition levels $E(-/0)$ and $E(0/+)$ below and above E_F, respectively, if the maximum fluctuation is greater than $U_{\text{eff}}/2$. The T_3^- defects form in regions of high potential and the T_3^+ defects form in regions of low potential. These results represent a new physical picture of the theory of Bar-Yam *et al.*[1] and unify many previously baffling experimental results. Charged dangling-bond de-

fects have important consequences for ESR, transport, and metastability in *a*-Si:H. There is considerable experimental evidence supporting the predictions of the potential fluctuation model for undoped *a*-Si:H, including distributions of dangling-bond transition levels and copious equilibrium T_3^+ and T_3^- defects.

Note added in proof. Yamasaki *et al.* [Phys. Rev. Lett. **65**, 756 (1990)] recently discovered additional evidence for charged dangling-bond defects in *a*-Si:H. They measure the hyperfine structure of the ESR and LESR signals and conclude that the $g=2.004$ LESR signal originates from a localized state similar to the T_3^0 dangling-bond orbital, most likely optically excited T_3^- or T_3^+ defects. The small difference in the g value between the native T_3^0 and the T_3^- or T_3^+ defects excited to T_3^0 could be due to their different hybridizations (as discussed in Sec. IV) or to their different positions in the gap.

ACKNOWLEDGMENTS

The authors are grateful to Thomas McMahon for clarifying conversations about *s* centers, and to Richard Crandall, Yaneer Bar-Yam, J. David Cohen, P. Craig Taylor, Mathieu Kemp, and Alex Zunger for many helpful discussions. David Alder greatly influenced our thinking. One of us (M.S.) acknowledges the Solar Energy Research Institute for financial support through a subcontract. This work was supported by the U.S. Department of Energy under Contract No. DE-AC02-83CH10093.

[1]Y. Bar-Yam, D. Adler, and J. D. Joannopoulos, Phys. Rev. Lett. **57**, 467 (1986).

[2]Z. E. Smith, in *Advances in Amorphous Semiconductors,* edited by H. Fritzsche (World Scientific, Singapore, 1988), p. 409,

[3]K. Winer, Phys. Rev. Lett. **63**, 1487 (1989); R. A. Street and K. Winer, Phys. Rev. B **40**, 6236 (1989); K. Winer, *ibid.* **41**, 12 150 (1990).

[4]B. I. Halperin and M. Lax, Phys. Rev. **148**, 722 (1966).

[5]H. Fritzsche, J. Non-Cryst. Solids **6**, 49 (1971).

[6]H. Overhof and W. Beyer, Philos. Mag. B **43**, 433 (1981).

[7]V. L. Bonch-Bruevich, Fiz. Tverd. Tela (Leningrad) **4**, 2660 (1962) [Sov. Phys.—Solid State **4**, 1953 (1963)].

[8]B. I. Shklovskii and A. L. Efros, *Electronic Properties of Doped Semiconductors* (Springer-Verlag, Heidelberg, 1984).

[9]E. N. Economou, in *Physics and Applications of Amorphous Semiconductors,* edited by F. Demichelis (World Scientific, Singapore, 1988), p. 3.

[10]S. D. Baronovskii and M. Silver, Philos. Mag. Lett. **61**, 77 (1990).

[11]M. Kemp (private communication) has calculated the (negligible) screening of the dipole potential when E_F lies in a continuous density of states of 10^{18} cm^{-3}. The screening is roughly one part in 10^6 at 10 Å from the dipole and along its axis.

[12]L. Ley, J. Reichardt, and R. L. Johnson, Phys. Rev. Lett. **49**, 1664 (1982).

[13]P. Kelfve, B. Blomster, H. Siegbahn, E. Sanhueza, and O. Goscinski, Phys. Scr. **21**, 75 (1980).

[14]B. Kramer, H. King, and A. MacKinnon, Physica B+C **117&118B**, 944 (1983); H. King, B. Kramer, and A. MacKinnon, Solid State Commun. **47**, 683 (1983).

[15]J. Baum, K. K. Gleason, A. Pines, A. N. Garroway, and J. A. Reimer, Phys. Rev. Lett. **56**, 1377 (1986).

[16]J. A. Reimer, private communication.

[17]K. Winer and M. Cardona, Solid State Commun. **60**, 207 (1986).

[18]F. R. Jeffrey, P. D. Murphy, and B. C. Gerstein, Phys. Rev. B **23**, 2099 (1981).

[19]A. H. Mahan, D. L. Williamson, B. P. Nelson, and R. S. Crandall, Phys. Rev. B **40**, 12 024 (1989).

[20]L. D. Landau and E. M. Lifschitz, *Electrodynamics of Continuous Media* (Pergamon, Oxford, 1960), p. 40.

[21]In one-dimensional potential fluctuations, such as a *p-n-p* structure or a random doping superlattice, the situation is more complex. The edge of the conduction-band density of states clearly follows the fluctuation, and this may correspond to a two-dimensional mobility edge for transverse dc conductivity. However, in the longitudinal direction, there is a unique, position-independent mobility edge for dc transport. In the *p-n-p* structure, for example, an *n*-layer eigenstate at the conduction-band edge may be extended in the transverse directions, but clearly is localized in the longitudinal direction. It cannot penetrate the potential barriers formed by the two adjacent *p* layers. Longitudinal electron conduction in this structure occurs at energies above the level of the *p*-layer conduction-band edge. This is the position-independent mobility edge.

[22]To treat thermopower in *a*-Si:H, Overhof and Beyer [*Electronic Transport in Hydrogenated Amorphous Silicon* (Springer-Verlag, Berlin, 1989), p. 113] introduce the concept of a local mobility edge which follows potential fluctuations when the fluctuation correlation length is an order of magnitude *longer* than the inelastic scattering length L_l. The observation [K. Hattori, T. Mori, H. Okamoto, and Y. Hamakawa, Phys. Rev. Lett. **60**, 825 (1988)] of quantum confinement effects in a 50 Å *a*-Si alloy superlattice suggests that L_l in *a*-Si:H is considerably greater than the correlation length of the dipolar potential fluctuations we are considering. For this reason, and because we compute energies relative to the dc-conductivity mobility edge, the concept of local mobility edge is irrelevant to the present discussion.

[23]Z E. Smith and S. Wagner, Phys. Rev. B **32**, 5510 (1985).

[24]R. A. Street, J. Kakalios, and T. M. Hayes, Phys. Rev. B **34**, 3030 (1986).

[25]T. J. McMahon and R. Tsu, Appl. Phys. Lett. **51**, 412 (1987).

[26]S. Zafar and E. A. Schiff, J. Non-Cryst. Solids **114**, 618 (1989).

[27]H. M. Branz, Phys. Rev. B **39**, 5107 (1989).

[28]W. Shockley and J. Moll, Phys. Rev. **119**, 1480 (1960).

[29]S. Froyen and A. Zunger, Phys. Rev. B **34**, 7451 (1986).

[30]H. M. Branz and M. Silver, in Amorphous Silicon Technology–1990, edited by A. Madan, M. J. Thompson, P. C. Taylor, P. G. LeComber, and Y. Hamakawa (Materials Research Society, Pittsburgh, in press).

[31]M. Stutzmann and W. B. Jackson, Solid State Commun. **62**, 153 (1987).

[32]Y. Bar-Yam and J. D. Joannopoulos, Phys. Rev. Lett. **56**,

2203 (1986).
[33]V. Heine, in *Solid State Physics,* edited by H. Ehrenreich, F. Seitz, and. D. Turnbull (Academic, New York, 1980), Chap. 1, pp. 92–96.
[34]D. Adler, Solar Cells **9**, 133 (1983).
[35]D. Adler, in *Semiconductors and Semimetals, Vol. 21A,* edited by J. I. Pankove (Academic, Orlando, 1984), p. 291.
[36]V. Cannella, J. McGill, Z. Yaniv, and M. Silver, J. Non-Cryst. Solids **77/78**, 1421 (1985).
[37]M. H. Brodsky and R. S. Title, Phys. Rev. Lett. **23**, 581 (1969).
[38]M. Stutzmann and D. K. Biegelsen, Phys. Rev. B **40**, 9834 (1989).
[39]R. A. Street and D. K. Biegelsen, J. Non-Cryst. Solids **35/36**, 651 (1980).
[40]T. Shimizu, H. Kidoh, A. Morimoto, and M. Kumeda, Jpn. J. Appl. Phys. **28**, 586 (1989).
[41]J. Ristein, J. Hautala, and P. C. Taylor, Phys. Rev. B **40**, 88 (1989).
[42]H. M. Branz, Phys. Rev. B **41**, 7887 (1990).
[43]J. M. Essick and J. D. Cohen, J. Non-Cryst. Solids **114**, 435 (1989); J. M. Essick and J. D. Cohen, Phys. Rev. Lett. **64**, 3062 (1990).
[44]E. A. Schiff, personal communication.
[45]J. G. Simmons and G. W. Taylor, Phys. Rev. B **4**, 502 (1971).
[46]D. L. Staebler and C. R. Wronski, Appl. Phys. Lett. **31**, 292 (1977).
[47]H. Dersch, J. Stuke, and J. Beichler, Appl. Phys. Lett. **38**, 456 (1981).
[48]R. S. Crandall, Phys. Rev. B **36**, 2645 (1987).
[49]P. E. Vanier and R. W. Griffith, J. Appl. Phys. **53**, 3098 (1982).
[50]P. D. Persans, Philos. Mag. B **46**, 435 (1982).
[51]T. J. McMahon and R. S. Crandall, Phys. Rev. B **39**, 1766 (1989).
[52]P. O'Connor and J. Tauc, Solid State Commun. **36**, 947 (1981).
[53]W. E. Spear, C. Cloude, D. Goldie, and P. G. LeComber, J. Non-Cryst. Solids **97/98**, 15 (1987).
[54]M. Silver, in Ref. 9, p. 28.
[55]L. Xu, G. Winborne, M. Silver, V. Cannella, and J. McGill, Philos. Mag. B **57**, 715 (1988).
[56]D. Goldie, P. G. LeComber, and W. E. Spear, Philos. Mag. Lett. **58**, 107 (1988).
[57]R. A. Street, Phys. Rev. B **21**, 5775 (1980).
[58]C. R. Wronski, B. Abeles, T. Tiedje, and G. D. Cody, Solid State Commun. **44**, 1423 (1982).
[59]J. Kocka, J. Non-Cryst. Solids **90**, 91 (1987).